Transient reduction of the drag coefficient of charged droplets via the convective reversal of stagnant caps

Brad S. Hamlin[1] and William D. Ristenpart[1,2]
[1]*Department of Chemical Engineering and Materials Science, University of California at Davis, Davis, California 95616, USA*
[2]*Department of Food Science and Technology, University of California at Davis, Davis, California 95616, USA*

(Received 22 September 2011; accepted 2 December 2011; published online 23 January 2012)

Droplets are frequently observed to move as if they were solid rather than liquid, i.e., with no slip at the liquid-liquid interface. This behavior is usually explained in terms of the so-called "stagnant cap" model, in which surfactants accumulate at the trailing edge of the droplet, immobilizing the surface and increasing the observed drag coefficient. Here, we show that the drag coefficient for charged droplets is temporarily reduced by reversing the direction of an electric driving force. Using high speed video, we simultaneously track the velocity and relative interfacial velocity of individual aqueous droplets moving electrophoretically through oil. The observed velocity behavior is highly sensitive to the concentration of surfactant. For sufficiently low or sufficiently high concentration, upon reversal of the electric field the droplet rapidly accelerates in the opposite direction but then decelerates, concurrent with a transient rearrangement of tracer particles on the droplet surface. In contrast, droplets with intermediate surfactant concentrations exhibit neither deceleration nor significant tracer particle rearrangement. We interpret the observations in terms of convectively dominated rearrangement of the stagnant cap, and we discuss the implications for precise electrophoretic control of droplet motion in lab-on-a-chip devices and industrial electrocoalescers. © *2012 American Institute of Physics*. [doi:10.1063/1.3674301]

I. INTRODUCTION

Stokes' classic result[1] for the viscous drag force on a sphere, $\mathbf{F}_{\text{drag}} = 6\pi\mu a\mathbf{U}$, is valid only for solid spheres in the limit of creeping flow. Because relative motion can occur at liquid/liquid interface, a different drag force is expected for liquid spheres. The first quantitative model was described independently a century ago by Hadamard[2] and Rybczynski.[3] By imposing continuity of shear and velocity at the liquid/liquid interface, they predicted that a spherical droplet or bubble of radius a moving at velocity $\mathbf{U}$ would experience a drag force

$$\mathbf{F}_{\text{drag}} = 4\pi\mu a\lambda\mathbf{U}. \tag{1.1}$$

Here, $\lambda = \frac{3\mu_i+2\mu}{2(\mu_i+\mu)}$ describes the effect of the viscosity contrast between the inside (μ_i) and outside (μ) of the sphere. In the limit, where $\mu_i \to 0$ (i.e., inviscid bubbles), $\lambda \to 1$ and the drag force is $4\pi\mu a\mathbf{U}$. In contrast, when $\mu_i \to \infty$ (i.e., a rigid sphere), $\lambda \to 3/2$ and Stokes' law is recovered. For otherwise identical spheres (same density and radius), the Hadamard-Rybczynski theory predicts a settling velocity up to 50% greater than Stokes' solution.

Early experiments on the sedimentation of droplets,[4] however, revealed a marked discrepancy between the observed and predicted droplet settling velocities, at least for droplets smaller than ~1 cm in diameter. In particular, droplets or bubbles containing minute amounts of surfactants (as small as 10^{-6} M) moved significantly slower than predicted by the Hadamard-Rybczynski solution.[5] Experiments with tracer particles demonstrated the existence of a so-called "stagnant cap" at the trailing end of the droplet, where the surface velocity vanishes.[6] Frumkin and Levich provided the first model consistent with this observation, in terms of a gradient in surfactant molecules induced

convectively along the surface of a droplet.[7,8] This concentration gradient causes a surface tension gradient, inducing a Marangoni stress that opposes the motion of the interface and ultimately leads to surface rigidification.

The stagnant cap model has been studied extensively both experimentally[5,6,9–15] and numerically[11,16–18] in various limiting cases. Davis and Acrivos[11] presented an early numerical solution in the simplified case of no adsorption or desorption of surfactants to or from the interface; an exact solution was later presented by Sadhal and Johnson.[19] Refinements to the model have included the addition of adsorption/desorption kinetics of surfactant to the interface[16] as well as the effects of droplet/bubble deformation.[17] Most experimental studies have focused on the steady rise velocities of bubbles[6,10,14,15] and droplets[4,6,9,10] for application in adsorption column design. More recently, Zhang and Finch measured the transient rise velocities of bubbles in the case of dilute surfactant concentrations, and they showed that the steady state rise velocity is independent of the bulk concentration of surfactant.[5] At higher surfactant concentrations, Stebe *et al*. showed that interfaces can "remobilize," if the surfactant has fast adsorption/desorption kinetics and if the surfactant concentration is sufficiently above the critical micelle concentration. In this situation, surfactant molecules are convectively forced to the trailing end of the droplet where they desorb and micellize. To replenish the surface, micelles on the leading end break apart and adsorb. This process prevents the formation of a gradient in surfactant concentration, so no Marangoni stress immobilizes the surface[20,21] and the drag coefficient predicted by the Hadamard-Rybczynski theory is observed.

Notably, all of the above experimental and numerical work on stagnant caps has focused on gravity or pressure driven flows. It has long been known,[22] however, that charged droplets also move electrophoretically. Many studies on the electrophoretic motion of droplets focus on electrolytic solutions where complicated electrokinetic effects can occur, as discussed in detail by Baygents and Saville.[23] If the surrounding liquid is sufficiently nonconductive, however, the Debye length κ^{-1} is very large compared to the droplet radius ($\kappa a \ll 1$) and the electrophoretic force on the droplet is simply $Q\mathbf{E}$, where Q is the droplet charge and $\mathbf{E}$ is the applied electric field.[24] A balance of this electrophoretic driving force against the viscous drag and gravitational force gives the droplet velocity; this balance was used by Millikan in his classic measurements of the elementary charge using charged oil droplets in air.[25]

Charged aqueous droplets in oil also move electrophoretically, but more complicated charge transfer effects can occur.[26–29] Specifically, in sufficiently large electric fields, a charged drop moves towards an oppositely charged electrode, and upon contact it becomes oppositely charged and moves back toward the other electrode. This process continues indefinitely, with the droplet shuttling charge between two electrodes by "bouncing" between them.[29] The observed velocities have been used to estimate the charge on a droplet by balancing the viscous and electrophoretic driving forces,[28–30] an approach predicated on the assumption that the viscous drag is well characterized and time invariant. Little is known, however, about the influence of the stagnant cap on the motion of charged drops, and no work to date has examined the effect of rapid changes on the direction of motion of stagnant caps.

In this paper, we demonstrate that the drag coefficient for charged droplets is temporarily reduced after a reversal in the electric field direction. We show that this drag reduction is highly sensitive to the type and concentration of surfactant in the droplet; drag reduction occurs at concentrations well below or well above the critical micelle concentration (CMC), but not at intermediate concentrations. Using tracer particles to visualize the droplet surface, we demonstrate that the drag reduction is commensurate with a convective time scale for stagnant cap formation and show that even when the droplet is already at a steady velocity, the drag can be temporarily reduced by changing the direction of motion. Finally, we discuss the implications for several applications involving charged drops, including charge estimation via single droplet velocimetry, precise electrophoretic control of droplet motion in lab-on-a-chip devices, and separation efficiency in industrial electrocoalescers.

II. EXPERIMENTAL METHODS

The experimental apparatus is sketched in Fig. 1 (left). Two spherical brass electrodes (each 6.5 mm diameter, separated by 5 mm) are placed in a polystyrene cuvette (12.5 mm ×

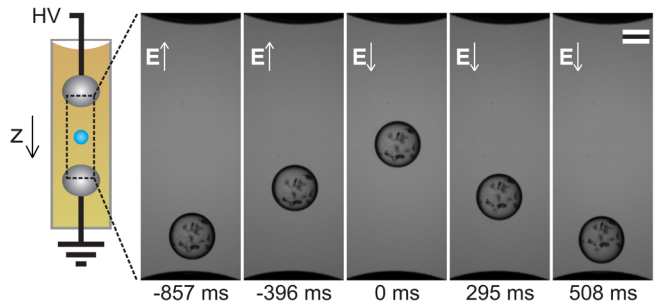

FIG. 1. (Color online) Left: Schematic of the experimental apparatus (not to scale). Right: Time lapse images of a 0.5 μl DI water droplet "bouncing" in response to a reversal in the applied electric field. Initially, the droplet moves upward electrophoretically shortly after touching the bottom electrode and acquiring charge. At $t = 0$, the polarity of the applied field is reversed, and the droplet moves downward. The surrounding fluid is 100 cS polydimethylsiloxane (PDMS) oil. The black spots on the droplet are phenolphthalein aggregates on the surface of the droplet. Scale bar is 0.5 mm.

12.5 mm × 45 mm) filled with 100 cS silicone oil (polydimethylsiloxane, Sigma Aldrich). A 0.5 μl droplet of water ($a \approx 0.45$ mm) with specified surfactant concentration is pipetted manually between the electrodes. Upon insertion, the droplet moves toward an electrode, whereupon it acquires charge and then begins "bouncing" back and forth between electrodes in a fashion similar to previous observations.[26–29] Spherical electrodes are convenient because the dielectrophoretic forces acting on the droplet[31] drive it to the maximum in the gradient in the field, which in this geometry lies on the line of closest separation between the spheres. In this way, the position of the droplet relative to the side walls of the cuvette is controlled, minimizing wall effects and simplifying the high speed photography. Silicone oil was chosen because of its extremely low conductivity, which helps to prevent charge leakage[32,33] from the aqueous droplet into the surrounding fluid. The characteristic charge relaxation time is $\tau = \frac{\epsilon}{\sigma}$, where ϵ is the oil permittivity and σ is its conductivity. For silicone oil, $\epsilon \approx 3\epsilon_0$, and $\sigma \approx 10^{-13}$ S/m, yielding $\tau \approx 100$ s.[34] In our experiments, the droplets typically move between electrodes in less than 1 s, so charge relaxation effects are negligible, and to a good approximation Q remains constant except when the droplet contacts an electrode.

To avoid complexities associated with increased viscous hindrance[35] and image charge attraction[36] when the droplet is in close proximity to the electrode surface, we developed an experimental procedure to switch the direction of the applied field when the droplet was far from either electrode, i.e., in "mid-flight" between the electrodes. Because the droplet charge is approximately constant, the direction of the electrophoretic force $Q\mathbf{E}$, and consequently the direction of motion, is controlled entirely by the sign of $\mathbf{E}$. From the observed velocities, we estimate that the drop charges are on the order of 10^{-11} C, which gives rise to an electrophoretic force roughly 5 times greater than the gravitational force. Electric potentials on the order of 1000 to 2000 V were generated by a Trek Model 610 E Cor-A-Trol high voltage supply, which has a relay switch that allows rapid reversal of the applied polarity on command. The time required for complete reversal of the field polarity was measured by tracking the current with a high-resolution electrometer and found to be approximately 3 ms, which is small compared to the time scale observed for changes in the droplet velocity (approximately 100 ms, cf. Fig. 2).

The velocity behavior of droplets subjected to a sudden reversal in the electric field direction was examined in droplets with three different surfactants: sodium dodecyl sulfate (SDS), Brij-35, and Triton X-100. SDS was chosen because it is a commonly used ionic surfactant, while Brij-35 and Triton X-100 were chosen as representative nonionic surfactants. For each surfactant, the concentration was varied from zero to well above the respective (CMC $= 8.2 \times 10^{-3}$ M, 6×10^{-5} M, and 2.4×10^{-4} M for SDS, Brij-35, and Triton X-100, respectively[37,38]).

The droplet motion was tracked using a high speed video camera (Phantom v7.3) at a frame rate of 1000 images per second. The videos were analyzed using standard image analysis techniques to track the droplet position versus time, and the trajectories were differentiated with a 5-point (5 ms) running average to obtain the velocity. To visualize the droplet surface velocity, 2 g/l of phenolphthalein was added to the surfactant solutions. Phenolphthalein is only sparingly soluble in both the water and the oil, so at low surfactant concentrations the phenolphthalein flocs rapidly assemble on the droplet surface. At higher surfactant concentrations, the flocs reside both

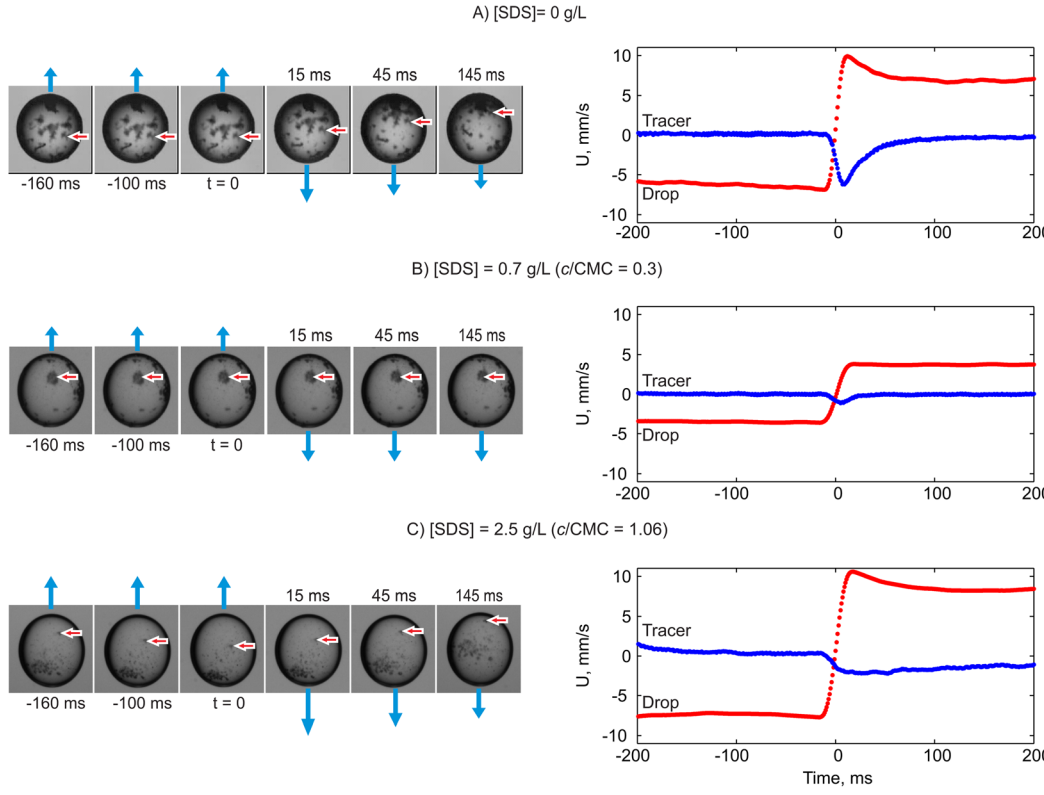

FIG. 2. (Color online) Representative droplet behavior in response to a sudden polarity reversal at $t = 0$ for three different SDS concentrations: (a) 0 g/l, (b) 0.7 g/l, and (c) 2.5 g/l. Time lapse images at left are centered on the droplet to emphasize the motion of the phenolphthalein tracer particles (dark spots). Horizontal arrows (red) highlight representative tracers, while vertical arrows (blue) qualitatively depict the direction and magnitude of the instantaneous droplet velocity. The plots at right show the corresponding droplet velocity and relative tracer velocity versus time. In each case, the applied potential difference is 1000 V; droplet diameters are approximately 1 mm (enhanced online) [URL: http://dx.doi.org/10.1063/1.3674301.1] [URL: http://dx.doi.org/10.1063/1.3674301.2] [URL: dx.doi.org/10.1063/1.3674301.3].

at the surface and inside the water droplet; presumably at high enough concentrations, the surfactant helps to stabilize the flocs in the aqueous phase. The velocity of phenolphthalein flocs at the drop surface was also extracted from the high speed video and measured with respect to the velocity of the droplet centroid. By comparing the velocity of the aggregates on the surface to that of the droplet itself, the relative surface velocity of the droplet was obtained.

III. RESULTS

The typical behavior of a charged droplet in response to a sudden change in the direction of the applied electric field is shown in the time lapse images in Fig. 1 (right). In this example, after contacting the bottom electrode, the droplet initially moved upward electrophoretically; at $t = 0$ the polarity was reversed and the droplet rapidly began moving downward. To the naked eye, the change in direction looked instantaneous, but analysis of the high speed video reveals more complex behavior. The detailed velocity behavior of three representative droplets with different surfactant concentrations is shown in Fig. 2. The time lapse images on the left show cropped views centered on the droplet to illustrate the tracer particle motion, while the graphs on the right show the absolute droplet velocity and the relative tracer velocity. Focusing first on the case of no added surfactant (Fig. 2(a) and supplementary movie #1 (Ref. 45)), we see that initially the droplet moved upward at an approximately constant velocity, as indicated qualitatively by the vertical arrows (blue) in the time lapse images and quantitatively in the velocity data at right. Notably, during this time period the tracer particles did not move measurably with respect to the drop center (Fig. 2(a) left, horizontal arrows (red)), suggesting the drop was translating as a rigid sphere. Following the reversal of the electric field at $t = 0$, the droplet changed direction and moved

downward at an initially high velocity which then decayed to a steady, lower magnitude. Concurrent with this velocity decay, the phenolphthalein tracer particles were observed to move in the opposite direction (with respect to the drop center). As the droplet reached a steady velocity, the tracer particles likewise slowed down relative to the drop center (Fig. 2(a) right). We emphasize that the tracer particles were essentially stationary with respect to the droplet center except for the transient rearrangement following the electric field reversal.

The observed droplet velocity behavior was highly sensitive to the surfactant concentration in the droplet. Fig. 2(b) shows the behavior of a droplet with an intermediate concentration of SDS, slightly below the CMC. The droplet initially moved upward at a steady velocity, and there was no measurable relative motion of the tracer particles. Upon reversal of the applied electric field, the droplet accelerated in the opposite direction in a manner qualitatively similar to the no surfactant case. Quantitatively, however, the velocity behavior was quite different; the droplet velocity did not decay appreciably (cf. Fig. 2(a)). Instead, the droplet velocity reached a maximum value and plateaued. The behavior of the tracer particles also differed significantly; a very slight and shortlived "bump" in the velocity occurred near $t = 0$, yielding a barely discernible displacement in the positions of the tracer particles (Fig. 2(b) and supplementary movie #2 (Ref. 45)). Inspection of the high speed video shows that the velocity bump occurred simultaneously with a small deformation of the droplet shape, i.e., the aspect ratio of the droplet momentarily decreased. This rapid deformation occurred whenever the surfactant concentration was near the CMC. Since surfactants are known to impart an elastic character to liquid interfaces[39,40] one possible explanation is that the rapid change in the direction of the driving force caused an elastic deformation of the droplet. The important point here, however, is that outside of this short-lived deformation; the droplet surface was effectively rigidified at intermediate surfactant concentrations.

At even higher surfactant concentrations, the velocity behavior again differed (Fig. 2(c) and supplementary movie #3 (Ref. 45)). Initially, the upward droplet velocity was steady, but in contrast to the behavior at lower SDS concentrations the tracer particles were observed to recirculate, suggesting that the surface of the droplet was in motion. Note that at the higher surfactant concentrations, a substantial fraction of the phenolphthalein flocs resided inside the droplet, allowing internal recirculation to be visualized. After the reversal of the field polarity, the droplet reversed direction and exhibited displayed a transient decay in velocity similar to the no added surfactant case. The tracer particles likewise reversed their direction of recirculation, with the absolute magnitude of their velocity decaying by approximately a third over a timescale commensurate with the droplet velocity decay.

Additional experiments indicated that the behavior discussed above is robust. For dilute or high surfactant concentrations, transient velocity decays occurred following a polarity reversal regardless of the initial polarity and regardless of which electrode was live or grounded. Likewise, the behavior was insensitive to the absolute distance of the droplet from the electrodes; transient velocity decays were observed even if the polarity was reversed while the droplet was in close proximity to an electrode, although quantitatively the magnitudes of the velocity decay differed (data not shown). The effects of increased viscous hindrance and image charge attraction complicate interpretation of near-electrode behavior, so we focus here on the "mid-flight" behavior far from the electrodes.

A convenient quantitative measure of the velocity behavior is the ratio of the maximum observed downward velocity following the field reversal, U_{max}, to the final steady downward velocity, U_{final}. This ratio was measured systematically as a function of SDS concentration for two different applied potentials (1000 and 1500 V). No phenolphthalein was added in these trials to focus solely on the effect of SDS. Several trends are apparent (Fig. 3). First, the velocity ratio follows a complicated nonmonotonic concentration dependence. At low SDS concentrations, the velocity ratio U_{max}/U_{final} is approximately 1.5, consistent with Fig. 2(a). As the SDS concentration is increased, the velocity ratio decreases, eventually reaching a minimum value close to 1 (indicating no change in velocity, cf. Fig. 2(b)) at concentrations approximately 20% of the CMC. As the concentration is increased further up to the CMC, the velocity ratio climbs back up to 1.5 (cf. Fig. 2(c)), but at even higher concentrations the velocity ratio begins to decrease again. A second major trend is that the velocity ratio is insensitive to the applied field strength. Increasing the magnitude of the field strength by 50% had little effect on the magnitude of the velocity ratio over the entire range of concentrations.

The number density and exact distribution of phenolphthalein flocs differed on each droplet (as seen in Fig. 2), so differences in floc density conceivably could affect the velocity behavior. Since similar velocity decays were observed with and without phenolphthalein (cf. Figs. 2(a) and 3), however, a key implication is that the presence of phenolphthalein is not responsible for the observed velocity decays. We tested this hypothesis more directly by systematically varying the concentration of phenolphthalein in deionized water droplets (Fig. 4). The phenolphthalein concentration was varied from 0 to 13.5 g/l, far above the typical phenolphthalein concentrations of 2-3 g/l used here. The velocity ratio U_{max}/U_{final} was found to be insensitive to phenolphthalein concentration over the range of concentrations tested, with velocity ratios averaging about 1.4. The observations suggest that the droplet deceleration is insensitive to phenolphthalein concentration. Notably, even droplets with no surfactant or phenolphthalein (i.e., pure deionized water) exhibited a velocity ratio of about 1.4, suggesting that surface active contaminants were present in the system (discussed in more detail below).

To test whether similar velocity behavior occurs with nonionic surfactants, we measured U_{max}/U_{final} over a wide range of concentrations of Triton X-100 and Brij-35 in deionized water at 1500 V applied potential (Fig. 5). Qualitatively the behavior is quite similar to that found with SDS, with velocity ratios close to 1.5 at very low surfactant concentrations, a decrease to 1 at intermediate concentrations closer to the CMC, and an increase again at even higher concentrations. In contrast to SDS, however, relatively little surfactant induced a decrease of the velocity ratio: concentrations as small as 10^{-3} times the CMC yielded a velocity ratio close to 1, as opposed to approximately 20% of the CMC for SDS. Also, with the nonionic surfactants, the velocity ratio was not observed to increase back up to 1.5 at higher concentrations, instead plateauing near values of 1.2 to 1.3.

Additional experiments for varied surfactant concentration, but with phenolphthalein tracer particles, were conducted to characterize the relative surface motion of the droplets. The observations are summarized qualitatively in Table I. At low concentrations, the surface motion is similar among the three surfactants studied; we observe a transient rearrangement of the surface following the reversal of the applied electric field, concurrent with a decrease from the peak velocity. Intermediate concentrations below the CMC were likewise similar between surfactants; we observed no appreciable relative surface motion and no droplet velocity decay. The behavior for Brij-35 and Triton X-100 is qualitatively different at higher concentrations, however, as we observe

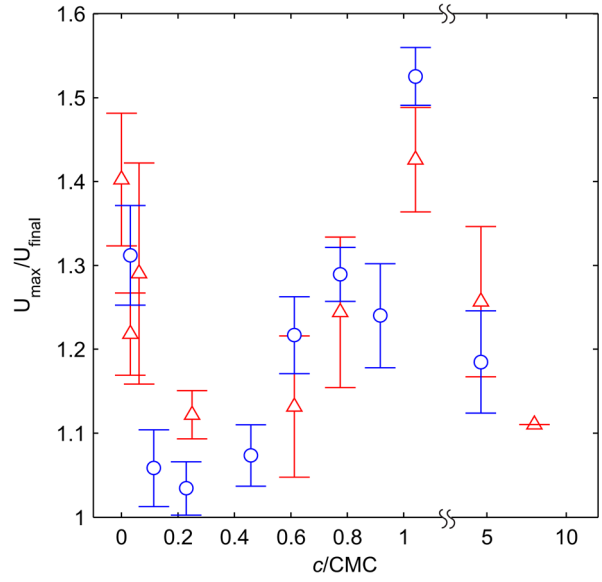

FIG. 3. (Color online) The effect of SDS concentration on the ratio of the peak velocity to the final velocity following a polarity reversal for two different applied electric potentials: circles (blue), 1000 V; triangles (red), 1500 V. Droplets were 0.5 μl deionized water with no phenolphthalein. Each point is the mean of 5 trials; error bars represent one standard deviation.

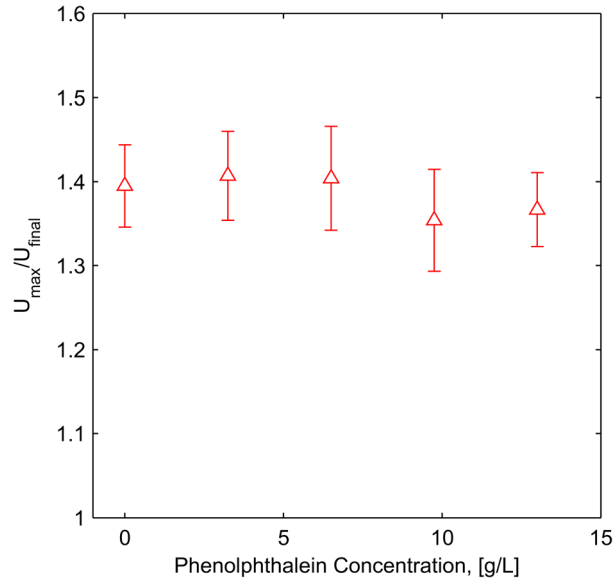

FIG. 4. (Color online) The effect of phenolphthalein concentration on the ratio of the peak velocity to the final velocity following a polarity reversal for 1 μl deionized water droplets with no added surfactant. The applied potential was 1500 V. Each point is the mean of 5 trials; error bars represent one standard deviation.

transient motion of the surface rather than the continuous recirculation exhibited by droplets with high concentrations of SDS.

IV. DISCUSSION

The experimental observations clearly demonstrate that droplets with sufficiently low or sufficiently high surfactant concentrations will decelerate significantly from a peak velocity following a sudden polarity reversal, and that the magnitude of the velocity decay is sensitive to the surfactant type and concentration. The key question is: why do the droplets decelerate?

Several physical effects are readily discounted. First, we note that the Reynolds number based on the droplet radius ranges from $\mathrm{Re} = 0.01$ to 0.05, so inertial effects should be negligible; even

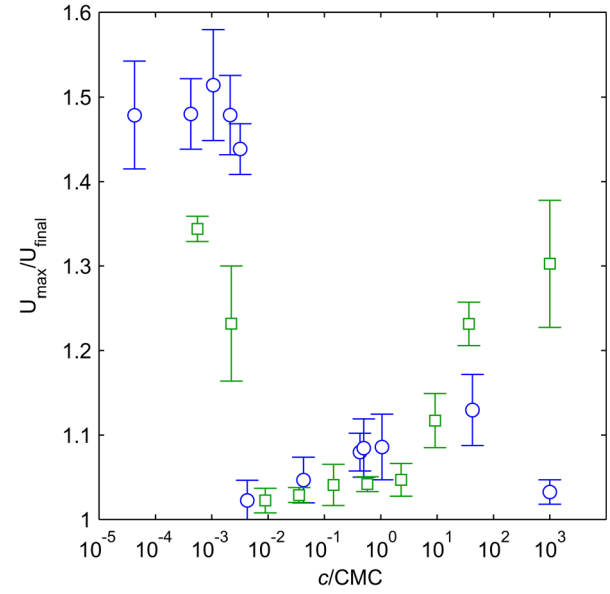

FIG. 5. (Color online) The effect of nonionic surfactant concentration on the ratio of the peak velocity to the final velocity following a polarity reversal at 1500 V: squares (green), Brij-35; circles (blue), Triton X-100. Droplets were 0.5 μl deionized water with no phenolphthalein. Each point is the mean of 5 trials; error bars represent one standard deviation.

TABLE I. Qualitative summary of tracer particle motion observed following a polarity reversal.

	$C \ll CMC$	$C < CMC$	$C \gtrsim CMC$	$C \gg CMC$
SDS	Transient surface motion	Immobilized surface	Transient surface motion	Continuous recirculation
Brij 35	Transient surface motion	Immobilized surface	Immobilized surface	Transient surface motion
Triton X-100	Transient surface motion	Immobilized surface	Immobilized surface	Transient surface motion

if inertial effects were significant, they would tend to inhibit acceleration in the opposite direction following the polarity reversal, rather than causing a deceleration in the new direction. A second possible explanation involves slow changes in the electric field polarity, i.e., the droplets simply move at a velocity determined by the instantaneous value of the electric field strength. Our electrometer measurements, however, indicate that the applied potential reaches a new steady value within 3 ms of reversal, which is small compared to the 100 ms time scale over which droplet deceleration and transient tracer particle rearrangement are observed. Moreover, a mechanism based on slow changes in the electric driving force is inconsistent with the observed dependence on the surfactant concentration.

A third and more subtle mechanism could involve electrical interactions with the electrodes, either through image charge or dielectrophoretic forces. Note that the image charge force is always attractive and scales as $Q^2/(2\,d)^2$, where d is the distance between the drop center and electrode surface; the dielectrophoretic force for our geometry is also attractive toward the electrode, with the force increasing in magnitude as d decreases. Straightforward scaling estimates suggest that the magnitude of the image charge and dielectrophoretic forces are negligible compared to the electrophoretic driving force when the droplet is near the midpoint between the electrodes. More importantly, both forces would cause an acceleration toward the electrode, rather than the observed deceleration.

The experimental observations instead suggest that the deceleration is associated with transient changes in the instantaneous drag coefficient. Notably, the ratio of the peak velocity to the final velocity is always observed to be within the range 1.5 to 1. For our droplets, the viscosity ratio is $\mu_i/\mu = 10^{-2}$, so $\lambda \approx 1$ and the ratio of the velocities for the Hadamard-Rybcynzki solution and the Stokes solution is also 1.5 to 1 (cf. Sec. I). The magnitude of the observed velocity decay is thus consistent with a transition between drag coefficients predicated on slip or no-slip, respectively, at the liquid/liquid interface. The tracer particle motion observed at low surfactant concentrations is consistent with this interpretation: the maximum tracer particle velocity occurs when the droplet velocity is maximal, and as the droplet decelerates to the final velocity, the tracer particle velocity concurrently decays to zero (cf. Fig. 2(a)).

If one posits the existence of a stagnant cap, then the observations at low surfactant concentration are explicable in terms of the transient relocation of the cap following the polarity reversal. For dilute surfactant concentrations, the change in direction of motion forces the stagnant cap to relocate to the other side of the droplet. During this transition, the droplet surface becomes temporarily mobile, allowing the droplet to "slip" through the oil at a higher velocity. A schematic of this proposed mechanism is shown in Fig. 6(a). The droplet initially moves at a steady velocity with a stagnant cap established on the trailing edge ($t < 0$), but after the droplet changes direction the surfactants relocate ($0 < t < a/U$) until the cap reforms at the opposite side of the droplet, again inhibiting recirculation within the drop ($t \gg a/U$).

We also observe a velocity decay and transient rearrangement when no surfactants are added, which would seem to suggest that no stagnant cap would be present and no velocity decay should be observed. It is well known, however, that surface active contaminants or impurities are difficult to entirely remove and that they readily serve to form stagnant caps; workers as early as Bond and Newton[4] observed behavior consistent with stagnant caps even with ostensibly "clean" liquids. Although the nature of the contaminants is unclear, the observed behavior is consistent with the dynamic rearrangement of a stagnant cap composed of surface active contaminants.

The stagnant cap mechanism is also qualitatively consistent with the behavior observed at intermediate surfactant concentrations. As the concentration is increased closer to the CMC, the cap increases in size until it subsumes the entire droplet, i.e., the "cap angle" is effectively 180°. In

this situation, the drop surface is effectively rigidified regardless of the direction of motion; in other words, the cap has nowhere to go because it already covers the surface (Fig. 6(b)). Accordingly, neither a velocity decay nor transient surface motion would occur following a polarity reversal, which is consistent with the experimental observations (cf. Fig. 2(b)). At even higher concentrations, more complicated effects associated with micellization and remobilization occur (discussed in more detail below).

The time scale over which the transient rearrangement occurs is consistent with a mechanism based on convectively dominated rearrangement of the stagnant cap. The conservation equation for the surfactant concentration Γ at the drop surface is

$$\frac{d\Gamma}{dt} + \mathbf{u}_s \cdot \nabla_s \Gamma = D_s \nabla_s^2 \Gamma + D_b \nabla c \cdot \vec{n} + \frac{D_s z e}{k_B T} \nabla_s \cdot (\Gamma \mathbf{E}), \tag{4.1}$$

where $\mathbf{u}_s$ is the local surface velocity, ∇_s denotes the surface gradient operator, D_s and D_b are the surface and bulk surfactant diffusivities, respectively, c is the bulk concentration, z is the valence of the ions, e is the elementary charge, k_B is the Boltzmann constant, and T is the temperature. The first two terms on the right-hand side of Eq. (4.1) represent diffusion along the surface and sorption into the surface, respectively, while the last term represents electromigration. Because of the coupling between both the flow field and the electric field, a full solution is challenging, but scaling estimates indicate that some of the terms are negligible for the experimental conditions investigated here. Selecting the droplet radius a as the characteristic length scale and the absolute drop velocity U as the characteristic velocity, nondimensionalization of Eq. (4.1) yields

$$\frac{d\hat{\Gamma}}{d\hat{t}} + \hat{\mathbf{u}}_s \cdot \hat{\nabla}_s \hat{\Gamma} = \frac{1}{Pe_s} \hat{\nabla}_s^2 \hat{\Gamma} + \frac{\hat{\chi}}{Pe_b} \hat{\nabla} \hat{c} \cdot \vec{n} + \frac{\hat{E}_0}{Pe_s} \hat{\nabla}_s (\hat{\Gamma} \hat{\mathbf{E}}), \tag{4.2}$$

where the various dimensionless terms are defined as

$$\mathrm{Pe}_s \equiv \frac{aU}{D_s}, \quad \mathrm{Pe}_b \equiv \frac{aU}{D_b}, \quad \hat{\chi} \equiv \frac{ac_b}{\Gamma_0}, \quad \hat{E}_0 \equiv \frac{zeaE_s}{k_b T}, \quad \hat{t} \equiv t\frac{U}{a}. \tag{4.3}$$

Here Γ_0 is the maximum possible surface concentration, c_b is the bulk concentration of surfactant, and E_s is the electric field strength along the droplet surface. Substitution of the characteristic values $a = 1$ mm, $U = 10$ mm/s, and $D_s = 10^{-11}$ m^2/s (Refs. 41 and 42) yields $\mathrm{Pe}_s = 10^6$, indicating that surface diffusion is negligible. The relative magnitude of the sorption term depends on $\hat{\chi}$, which gauges the relative magnitudes of the bulk surfactant concentration and maximum surface concentration.

As for electromigration, we first note that z is effectively zero for nonionic surfactants, so electromigration is negligible. For ionic surfactants (e.g., SDS), we obtain an approximate estimate for E_s by assuming the droplet and surrounding oil are perfect dielectrics, so that the classical result for a sphere in a uniform electric field pertains,[36] viz.,

$$E_s = \frac{3}{\epsilon_w/\epsilon_o + 2} E_\infty. \tag{4.4}$$

Here, $\epsilon_w = 78$ and $\epsilon_o = 3$ are the dielectric constants of the water and the oil, respectively. We estimate the field strength as $E_\infty \approx \Phi_{app}/d$, where Φ_{app} is the applied potential and d is the electrode separation. With these estimates, even for applied field strengths as high as 300 V/mm, the dimensionless field strength is only $\hat{E}_0 \approx 200$, so the ratio $\hat{E}_0/\mathrm{Pe}_s$ is negligibly small. Thus, to a good approximation, the surfactant concentration on the drop surface is governed by

$$\frac{d\hat{\Gamma}}{d\hat{t}} + \hat{\mathbf{u}}_s \cdot \hat{\nabla}_s \hat{\Gamma} = \frac{\hat{\chi}}{Pe_b} \hat{\nabla} \hat{c} \cdot \vec{n}. \tag{4.5}$$

A key implication is that in the limit of small bulk surfactant concentrations ($c \to 0$), the influence of sorption is negligible and the surfactant concentration (and consequent Marangoni stress) is

governed completely by convective forces. Notably, substitution of the characteristic magnitudes $a = 1$ mm, $U = 10$ mm/s yields a convective time scale of 100 ms, which is commensurate with the time scale over which the velocity is observed to decay experimentally (cf. Fig. 2).

At large bulk surfactant concentrations, in contrast, $\hat{\chi}$ increases in value, and a more complicated interaction between the bulk and the surface occurs. At values near and above the CMC (Fig. 6(c)), the droplet velocity decays from a maximal velocity (similar to the case of low

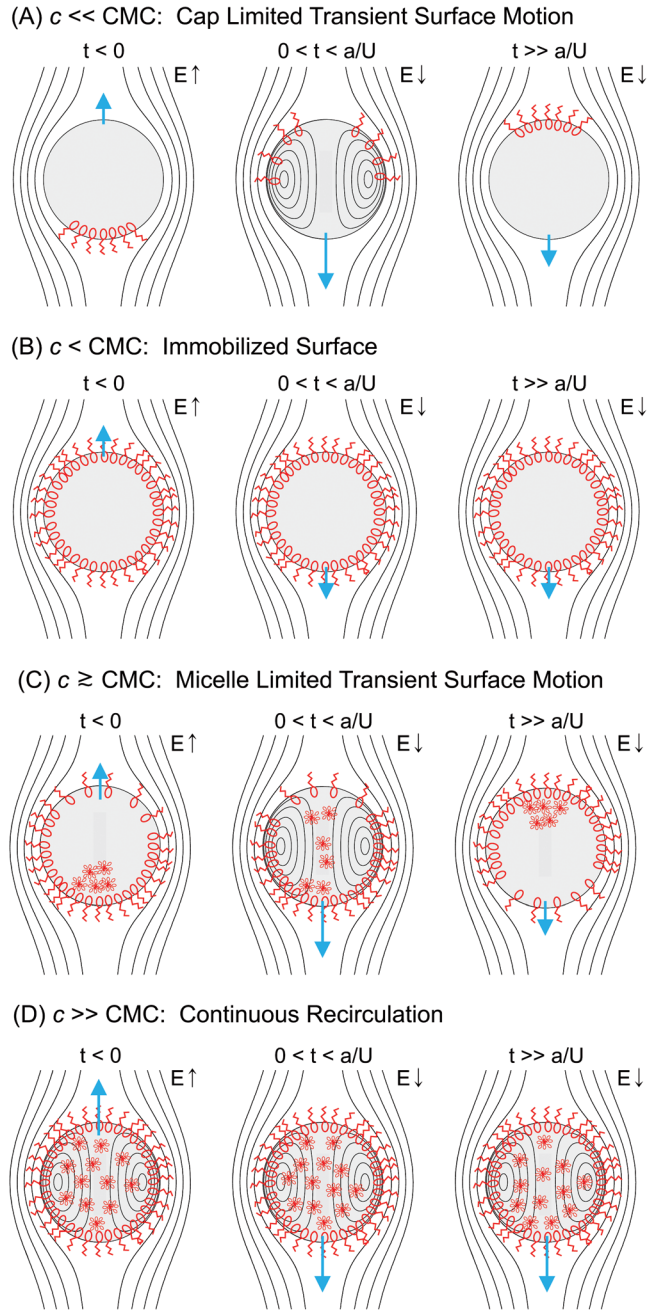

FIG. 6. (Color online) Schematic of the proposed mechanisms driving the velocity behavior following a polarity reversal. Arrows (blue) qualitatively indicate direction and magnitude of the droplet velocity. (a) At low concentrations, a stagnant cap transiently relocates, allowing the droplet to momentarily slip through the surrounding fluid at a higher speed. (b) At concentrations closer to the CMC, the stagnant cap covers the droplet, and the surface is effectively rigidified regardless of direction. (c) At concentrations near or above the CMC, an asymmetry in the micelle concentration within the bulk of the droplet transiently reverses, again allowing the droplet to slip through the surrounding fluid at a higher speed. (d) At very high concentrations, the gradient in micelle concentration vanishes and continuous recirculation is observed.

surfactant concentration). We hypothesize that this decay at high surfactant concentrations is caused by an asymmetry in micellar concentration inside the droplet, rather than a gradient along the surface. As discussed in detail by Stebe *et al.*,[20,21] as a droplet moves an asymmetry is formed in the local micellar concentration at the leading and trailing edges of the drop. The convective shear pulls surfactant monomers to the trailing edge, where they micellize to maintain the local monomer concentration in the bulk at the CMC. At the leading edge, micelles break apart to replenish the surface. If there is an asymmetry in the rates of adsorption and desorption at the leading and trailing edges of the droplet, then a local depletion of micelles and corresponding stagnant cap will form. If the micelle sorption kinetics are fast compared to convection, then increasing the surfactant concentration further (Fig. 6(d)) prevents local depletion of micelles and again remobilizes the surface. This latter behavior is consistent with the observed decrease in velocity ratio observed at very high SDS concentrations (cf. Fig. 3).

V. CONCLUSIONS

In this work, we demonstrated that a transient velocity decay can occur when charged droplets are subjected to a sudden change in the applied electric field direction. The magnitude of the velocity decay is highly sensitive to the surfactant type and concentration, but insensitive to the electric field strength. The observed time scale of the velocity decay, the observed surface motion and the surfactant concentration dependence are all consistent with a mechanism based on the convectively dominated rearrangement of a stagnant cap. Although the mechanisms presented in Fig. 6 are qualitatively in accord with the experimental observations, several details remain to be explained. For example, surface immobilization occurred at widely differing values of the surfactant concentration for the different surfactant types: $c/CMC \approx 10^{-3}$ for Brij-35 and Triton X-100, but $c/CMC \approx 10^{-1}$ for SDS. Likewise, full remobilization and recirculation was observed at sufficiently high SDS concentrations but was not observed for the non-ionic surfactants. Since this behavior presumably depends sensitively on the adsorption/desorption kinetics of the individual surfactants, more detailed numerical calculations will be helpful in interpreting these effects.

Regardless of the underlying details, the observations reported here have several implications for practical applications. First, precise control of the location of charged droplets in lab-on-a-chip devices[28,30] will most easily be accomplished at intermediate surfactant concentrations where no velocity decay occurs. If surfactants are undesired, then care must be taken into account for the transient velocity decrease following any changes in direction. Likewise, simulations of droplet motion within electrostatic separators or electrocoalescers[43] should take into account the non-uniform velocity following contact with an electrode or another drop;[29] a fascinating question involves the effect of the stagnant cap rearrangement on the dynamics of the Taylor cone formed when a droplet approaches an electrode or another droplet.[44] Most importantly, the results presented here highlight the need to fully characterize the drag on a droplet before using its observed velocity to estimate the charge, since errors of 50% could easily occur simply by assuming Stokes drag. Drag characterization experiments of the kind presented here should be conducted whenever precise charge measurements are necessary.

ACKNOWLEDGMENTS

We thank the American Chemical Society Petroleum Research Fund and the National Science Foundation (CAREER Grant No. CBET-1056138) for support, and we thank Professor In Seok Kang for suggesting phenolphthalein flocs as tracer particles.

[1]G. G. Stokes, "On the effect of the internal friction of fluids on the motion of pendulums," Trans. Cambridge Philos. Soc. **9**, 8 (1851).
[2]J. S. Hadamard, "Mouvement permanent lent d'une sphere liquide et visqueuse dans un liquide visqueux," C. R. Acad. Sci. **152**, 1735 (1911).
[3]W. Rybczynski, "Über die fortschreitende bewegung einer flssigen kugel in einem zhen medium," Bull. Acad. Sci. Cracovi, Ser. A 40 (1911).
[4]W. N. Bond and D. A. Newton, "Bubbles, drops, and Stokes' law (Paper 2)," Philos. Mag. **5**(30), 794 (1928).
[5]Y. Q. Zhang and J. A. Finch, "A note on single bubble motion in surfactant solutions," J. Fluid Mech. **429**, 63 (2001).
[6]R. Clift, J. R. Grace, and M. E. Weber, *Bubbles, Drops, and Particles* (Academic, New York, New York, 1978).

[7]A. Frumkin and V. Levich, "O vliyanii poverkhnostno-aktivnykh veshchestv na dvizhenie na granitse zhidkikh sred," Zh. Fiz. Khim. **21**(10), 1183 (1947).
[8]V. Levich, *Physicochemical Hydrodynamics* (Prentice-Hall, Englewood, New Jersey, 1962).
[9]P. Savic, "Circulation and distortion of liquid drops falling through a viscous medium," Report No. MT-22, (National Research Council Canada, 1953).
[10]R. M. Griffith, "The effect of surfactants on the terminal velocity of drops and bubbles," Chem. Eng. Sci. **17**(12), 1057 (1962).
[11]R. E. Davis and A. Acrivos, "The influence of surfactants on the creeping motion of bubbles," Chem. Eng. Sci. **21**(8), 681 (1966).
[12]W. S. Huang and R. C. Kintner, "Effects of surfactants on mass transfer inside drops," AIChE J. **15**(5), 735 (1969).
[13]J. F. Harper, "Bubbles with small immobile adsorbed films rising in liquids at low Reynolds-numbers," J. Fluid Mech. **58**(MAY8), 539 (1973).
[14]R. B. Fdhila and P. C. Duineveld, "The effect of surfactant on the rise of a spherical bubble at high Reynolds and Peclet numbers," Phys. Fluids **8**(2), 310 (1996).
[15]Y. Liao and J. B. McLaughlin, "Bubble motion in aqueous surfactant solutions," J. Colloid Interface Sci. **224**(2), 297 (2000).
[16]B. Cuenot, J. Magnaudet, and B. Spennato, "The effects of slightly soluble surfactants on the flow around a spherical bubble," J. Fluid Mech. **339**, 25 (1997).
[17]S. Tasoglu, U. Demirci, and M. Muradoglu, "The effect of soluble surfactant on the transient motion of a buoyancy-driven bubble," Phys. Fluids **20**(4), 040805 (2008).
[18]M. Fukuta, S. Takagi, and Y. Matsumoto, "Numerical study on the shear-induced lift force acting on a spherical bubble in aqueous surfactant solutions," Phys. Fluids **20**(4), 040704 (2008).
[19]S. S. Sadhal and R. E. Johnson, "Stokes-flow past bubbles and drops partially coated with thin-films. Part 1. Stagnant cap of surfactant film-exact solution," J. Fluid Mech. **126**(JAN), 237 (1983).
[20]K. J. Stebe, S. Y. Lin, and C. Maldarelli, "Remobilizing surfactant retarded fluid particle interfaces. 1. Stress-free conditions at the interfaces of micellar solutions of surfactants with fast sorption kinetics," Phys. Fluids A **3**(1), 3 (1991).
[21]K. J. Stebe and C. Maldarelli, "Remobilizing surfactant retarded fluid particle interfaces. 2. Controlling the surface mobility at interfaces of solutions containing surface-active components," J. Colloid Interface Sci. **163**(1), 177 (1994).
[22]G. Quincke, "Über die Fortführung materieller Theilchen durch strömende Elecktricität," Pogg. Ann. **113**, 513 (1861).
[23]J. C. Baygents and D. A. Saville, "Electrophoresis of drops and bubbles," J. Chem. Soc., Faraday Trans. **87**(12), 1883 (1991).
[24]W. B. Russel, D. A. Saville, and W. R. Schowalter, *Colloidal Dispersions* (Cambridge University Press, Cambridge, UK, 1989).
[25]R. A. Millikan, "On the elementary electrical charge and the Avogadro constant," Phys. Rev. **2**(2), 109 (1913).
[26]T. Mochizuki, Y. H. Mori, and N. Kaji, "Bouncing motions of liquid-drops between tilted parallel-plate electrodes," AIChE J. **36**(7), 1039 (1990).
[27]M. Hase, S. N. Watanabe, and K. Yoshikawa, "Rhythmic motion of a droplet under a dc electric field," Phys. Rev. E **74**(4), 046301 (2006).
[28]Y. M. Jung, H. C. Oh, and I. S. Kang, "Electrical charging of a conducting water droplet in a dielectric fluid on the electrode surface," J. Colloid Interface Sci. **322**(2), 617 (2008).
[29]W. D. Ristenpart, J. C. Bird, A. Belmonte, F. Dollar, and H. A. Stone, "Non-coalescence of oppositely charged drops," Nature **461**(7262), 377 (2009).
[30]D. J. Im, J. Noh, D. Moon, and I. S. Kang, "Electrophoresis of a charged droplet in a dielectric liquid for droplet actuation," Anal. Chem. **83**(13), 5168 (2011).
[31]H. A. Pohl, *Dielectrophoresis* (Cambridge University Press, Cambridge, UK, 1978).
[32]A. Khayari and A. T. Perez, "Charge acquired by a spherical ball bouncing on an electrode: Comparison between theory and experiment," IEEE Trans. Dielectr. Electr. Insul. **9**(4), 589 (2002).
[33]A. T. Perez, "Charge and force on a conducting sphere between two parallel electrodes," J. Electrost. **56**(2), 199 (2002).
[34]*Polymer Data Handbook*, edited by J. E. Mark (Oxford University Press, New York, New York, 1999).
[35]J. Happel and H. Brenner, *Low Reynolds Number Hydrodynamics* (Noordhoff International Leyden, The Netherlands, 1973).
[36]J. Jackson, *Classical Electrodynamics*, 3rd ed. (John Wiley and Sons, Hoboken, New Jersey, 1999).
[37]P. Mukerjee and K. J. Mysels, "Critical micelle concentrations of aqueous surfactant systems," U.S. National Bureau of Standards NSRDS-NBS 36 (U.S. Govt. Print. Off., Washington, 1971).
[38]S. Hait and S. Moulik, "Determination of critical micelle concentration (CMC) of nonionic surfactants by donor-acceptor interaction with Iodine and correlation of CMC with hydrophile-lipophile balance and other parameters of the surfactants," J. Surfactants Deterg. **4**(3), 303 (2001).
[39]S. T. Milner and S. A. Safran, "Dynamic fluctuations of droplet microemulsions and vesicles," Phys. Rev. A **36**(9), 4371 (1987).
[40]H. Gang, A. H. Krall, and D. A. Weitz, "Thermal fluctuations of the shapes of droplets in dense and compressed emulsions," Phys. Rev. E **52**(6), 6289 (1995).
[41]R. M. Weinheimer, D. F. Evans, and E. L. Cussler, "Diffusion in surfactant solutions," J. Colloid Interface Sci. **80**(2), 357 (1981).
[42]D. C. Clark, R. Dann, A. R. Mackie, J. Mingins, A. C. Pinder, P. W. Purdy, E. J. Russell, L. J. Smith, and D. R. Wilson, "Surface diffusion in sodium dodecyl sulfate-stabilized thin liquid films," J. Colloid Interface Sci. **138**(1), 195 (1990).
[43]J. S. Eow, M. Ghadiri, A. O. Sharif, and T. J. Williams, "Electrostatic enhancement of coalescence of water droplets in oil: A review of the current understanding," Chem. Eng. J. **84**(3), 173 (2001).
[44]J. C. Bird, W. D. Ristenpart, A. Belmonte, and H. A. Stone, "Critical angle for electrically driven coalescence of two conical droplets," Phys. Rev. Lett. **103**(16), 164502 (2009).
[45]See supplementary material at http://dx.doi.org/10.1063/1.3674301 for a description of each movie.